Article

Temperature Stable Compelled Composite Superhydrophobic Porous Coordination Polymers Achieved via Unattainable De novo Synthetic Method

Koya Prabhakara Rao, Masakazu Higuchi, Suryachandram Jettiboina, and Susumu Kitagawa

J. Am. Chem. Soc., **Just Accepted Manuscript** • DOI: 10.1021/jacs.8b07577 • Publication Date (Web): 29 Sep 2018

Temperature Stable Compelled Composite Superhydrophobic Porous Coordination Polymers Achieved *via* Unattainable *De novo* Synthetic Method

Koya Prabhakara Rao[†§*], Masakazu Higuchi[†], Jettiboina Suryachandram[§], and Susumu Kitagawa[†*]

†Institute for Integrated Cell-Materials Science (iCeMS), Kyoto University, Katsura, Nishikyo-ku, Kyoto 615-8510, Japan

†Department of Synthetic Chemistry and Biological Chemistry, Graduate School of Engineering, Kyoto University, Katsura, Nishikyo-ku, Kyoto 615-8510, Japan

[§]New Generation Materials Lab (NGML), Department of Science and Humanities, Vignan's Foundation for Science Technology and Research (VFSTR) University, Vadlamudi-522 213, Guntur, Andhra Pradesh, India

Supporting Information

ABSTRACT: We demonstrate a new *de novo* synthetic methodology to achieve high temperature stable compelled composite superhydrophobic porous coordination polymers (PCPs). These new PCPs achieved based on coordination capabilities of 1st-row transition metal ions like $\mathbf{Co^{2+}}$, $\mathbf{Ni^{2+}}$, and $\mathbf{Zn^{2+}}$. The obtained composite PCPs containing, $\mathbf{[Zn_2M_2O]^{6+}}$ (**M** = **Co** or **Ni**) bimetallic cluster core with open metal sites (OMSs), exhibited distinct iso-steric heats of adsorption and surface areas due to the difference in their open metal Lewis acidic sites of solvent-free state. Additionally, these composite PCPs, exhibit remarkable superhydrophobic properties with contact angles of 159.3 ° and 160.8°, respectively for **Zn-Co** and **Zn-Ni** analogs. This superhydrophobic surface survives even at high temperature for longer time periods. As projected, these new composite PCPs exhibits better surface area and heats of adsorption compared to **PESD–1 (Zn)** analogue due to more number of OMSs. Moreover, they display selective adsorption towards aromatic solvents like benzene and toluene over aliphatic solvents like cyclohexane due to corrugated and terminated aromatic hydrocarbon moieties towards the interactive surface. They also exhibit oil spill cleanup from the water surface in the powder form as well as pellet form up to 385 wt%. This study certainly offers a roadmap for designing and engineering of new composite superhydrophobic porous materials for better water and thermal stability along with OMSs. This type of PCPs exhibits the wide range of applications especially in catalysis, separation technology and securing the environmental problems like oil spill cleanup in from the sea water.

INTRODUCTION

Metal-organic frameworks (MOFs) which are also known as porous coordination polymers (PCPs) are emerged[1] as potential materials of the decade due to numerous applications in surface technology. Revolution of MOFs/PCPs has come due to their designable functionality[2, 3] according to the requirement, compared with conventional porous materials, such as activated carbon, zeolite, and related porous materials. The functionality in PCPs could be achieved mainly in two different parts of the PCP compounds. It could be at the ligand part[2] and at the metal cluster core part.[3] In the literature potentiality of reduced symmetry linkers has been reported[4]; having one type of coordinating group in different chemical environments offers the potential to expose new regions of phase space.[4] This enables to discover novel materials with feasible of innovative metal–oxygen–metal (M–O–M) clusters.

It is well-known that inorganic back bone (M–O–M linkage clusters) of the PCPs plays a vital role in their thermal and chemical stability.[5] In many cases, the inorganic moiety could be just a metal, after removal of the guest-solvent molecules lead to collapse of the structure or shows very low thermal stability.[6] Recently, we have reported[7], an asymmetrical ligand, Benzene-1,3,5-tris(*m*-Benzoic acid) (**H_3BTMB**) based first superhydrophobic PCP with external surface design (**PESD–1**) and a dense I^1O^3 superhydrophobic framework, **Pb[(H-BTMB)(DMF)]** exhibits selective adsorption of CO_2. In fact, these two PCPs possess superhydrophobicity due to highly corrugated aromatic hydrocarbon surface directed towards the guest species along with unique type of open metal sites (OMSs).

MOFs/PCPs containing OMSs display promising applications[8, 9] especially in catalysis, gas separation and storage. Particularly, OMSs play a substantial role in gas separation technology, where a particular gas can strongly captivate with a particular type OMSs.[9] In fact, many MOFs/PCPs reported in the literature were lack of OMSs after the evacuation of guest molecules. Nevertheless, in some MOFs/PCPs, metal clusters and/or metal ions coordinated to solvent molecules in as-synthesized form and they could be ambiguous after the evacuation of the guest molecules.[6] In reality, OMSs could not generate in many PCPs even after activation by removal of solvent molecules, because they fill coordination spaces without bonding to metals. In some PCPs, metals coordinated by solvent molecules could be converted to unstable OMSs after removal of the molecules. In this context, construction of PCPs

with stable OMSs is a precious approach for various applications in the field of porous materials. In this present study, we focused on functionalization of PCPs at a metal cluster core part (composite PCPs) for more open metal sites (OMSs) by choosing high coordination ability (Co^{2+} and Ni^{2+}) transition metal ions in place of four-coordination of Zn^{2+} ion in **PESD–1** PCP. These new composite PCPs expected to display more OMSs along with high water stability (superhydrophobicity) and good thermal stability (due to bimetallic cluster core).

Herein, we report a *de novo* synthetic method for the synthesis of composite PCPs, **PESD–2&3**, $[Zn_2M_2(\mu_3\text{-}OH)_2(BTMB)_2]$ (M = **Co** and **Ni**). The oxo-clusters in the pristine phases of **PESD–2&3**⊃Guest have converted to $[Zn_2M_2O]^{6+}$ (**M** = **Co** and **Ni**) clusters with OMSs in their degassed phases by losing a water molecule. Additionally, these new composite PCPs exhibit outstanding superhydrophobic properties compared to other M_4O cluster contained MOFs[10] (hygroscopic) reported in the literature.

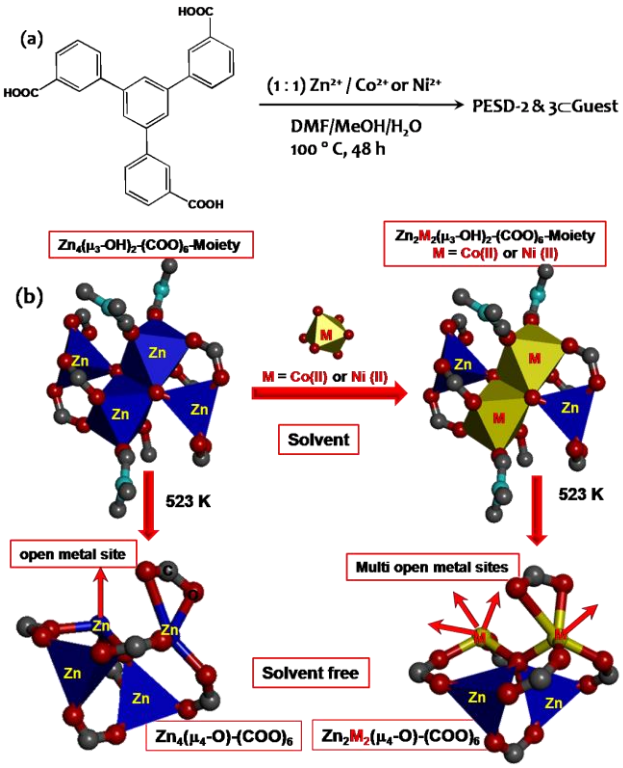

Scheme 1. (a) Synthesis of Composite **PESD–2&3**⊃Guest PCPs, (b) Schematic representation of the synthesis of composite porous coordination polymers with solvent and without solvent coordination environment.

RESULTS AND DISCUSSION

Syntheses

After successful achievement of first superhydrophobic PCP, **PESD–1⊃Guest**[7(a)], in which the $[Zn_4(\mu_3\text{-}OH)_2]^{6+}$ cluster core with OMSs is provocative part of the PCP for applications like gas separation and catalysis. In fact, the $[Zn_4(\mu_3\text{-}OH)_2]^{6+}$ cluster core changes to $[Zn_4O]^{6+}$ reversible by losing a H_2O molecule in degassed phase and vice versa by exposing OMS on Zn^{2+} is very peculiar and contrast to reported M_4O cluster contained MOFs (no OMSs).[10] These unique properties like Superhydrophobicity and OMSs together in single PCP of **PESD–1**, are invigorated for other analogs of this PCP. Consequently, we focused on the synthesis of **PESD–1**, analogs using other divalent transition metals in order to increase the number of OMSs for selective interactions with various gas molecules. We screened for all the first-row transition elements using similar solvo-thermal conditions employed for **PESD–1**⊃Guest along other possible methods. However, we could not able to synthesize any analogue of **PESD–1**, with one single metal alone at all four metal centers of $Zn_4(\mu_3\text{-}OH)_2]^{6+}$ cluster. It could be due to, first row transition metals prefers six-coordination (except **Zn**). In this context, we thought of introducing various M^{2+} ions specifically at the two octahedral-coordinating Zn^{2+} ion sites of $[Zn_4(\mu_3\text{-}OH)_2]^{6+}$ oxo-cluster (Scheme 1(b)). The other two tetrahedral-coordinating Zn^{2+} ions are retained in the structure and chemical formula, which is useful to stabilize the structure. Recently, bimetallic PCPs with M_4O clusters having four-coordination were synthesized by soaking single crystals consisting of one metal into a solution of another metal ion.[3a] We employed a different approach of a direct solvo-thermal synthetic approach based on our hypothesis that 1st-row divalent transition metal ions (except Zn^{2+}) could occupy only at an octahedral position. By this method, we could successfully introduce Co^{2+} and Ni^{2+} ions precisely at octahedral Zn^{2+} ion site of $[Zn_4(\mu_3\text{-}OH)_2]^{6+}$oxo-cluster (Scheme 1b) to synthesize the present composite, **PESD–2** & **3**⊃Guest PCPs.

PESD–2&3⊃Guest, $[Zn_2M_2(\mu_3\text{-}OH)_2(BTMB)_2(DMF)_3(MeOH)]\cdot(DMF)_2(H_2O)_2(MeOH)$ (M = **Co** and **Ni**) compounds synthesized by mixing, $Zn(NO_3)_2{\cdot}4H_2O/M(NO_3)_2{\cdot}6H_2O$ (M = **Co** and **Ni**) metal salts and H_3BTMB ligands,[11] in mixed solvent of DMF/MeOH/H_2O (2:1:1) at 100 °C (Scheme 1a). By utilizing X-ray florescence (XRF) analysis and changing the salts ratio of $Zn(NO_3)_2{\cdot}4H_2O$ and $M(NO_3)_2{\cdot}6H_2O$ (M = **Co** and **Ni**) in the starting reaction mixture, the desired ratio of **Zn** to **Co** or **Ni** (≈1:1) was achieved in the final product (see experimental section and SI for details).

X-Ray Crystal Structures

The **PESD–2&3**⊃Guest characterized by single crystal X-ray diffraction (XRD) analysis and found that they are iso-structural with **PESD–1** ⊃Guest[7] (Table S1, Figure 1, Figure S1 & S2). The μ_3-bridged hydroxyl proton refined by single crystal XRD analysis and confirmed by FTIR spectroscopic studies which observed a characteristic peak at around 3615 cm^{-1}, as shown in Figure S3. For example, single crystal structure of **PESD–2** ⊃Guest projected in figure 1. They have two-dimensional (**2D**) structure with (8,6) net topology,[7a] and form 1D channels along *b*-axis similar to **PESD–1**⊃Guest.[7a] Each of the individual layers comprised rhombus-shaped $[Zn_2M_2(\mu_3\text{-}OH)_2]^{6+}$ (**M** = **Co** and **Ni**) tetra-nuclear clusters that were mutually connected via the $BTMB^{3-}$ ligands to form an (8,6) net.[12] As shown in figure 1b, the $[Zn_2M_2(\mu_3\text{-}OH)_2]^{6+}$ cluster containing two octahedral M^{2+} ions (**M** = **Co** and **Ni**) and two tetrahedral Zn^{2+} ions and two μ_3-hydroxyl moieties (OH^-) that presented within the three-atom

mean planes formed by the metal centers. The octahedral M^{2+} (**M** = **Co** and **Ni**) ions coordinated to an oxygen atom of the three different carboxylate groups, two OH^- fragments and a solvent molecule. Whereas, the tetrahedral Zn^{2+} ions were coordinated to oxygen atoms of three different carboxylate moieties along with only one of the OH^- group. Even though within the $[Zn_2M_2(\mu_3\text{-}OH)_2(BTMB)_2]$ (**M** = **Co** and **Ni**) layers were comparatively dense, the voids formed between any two adjacent layers are large enough to accommodate all kinds of the guest species.

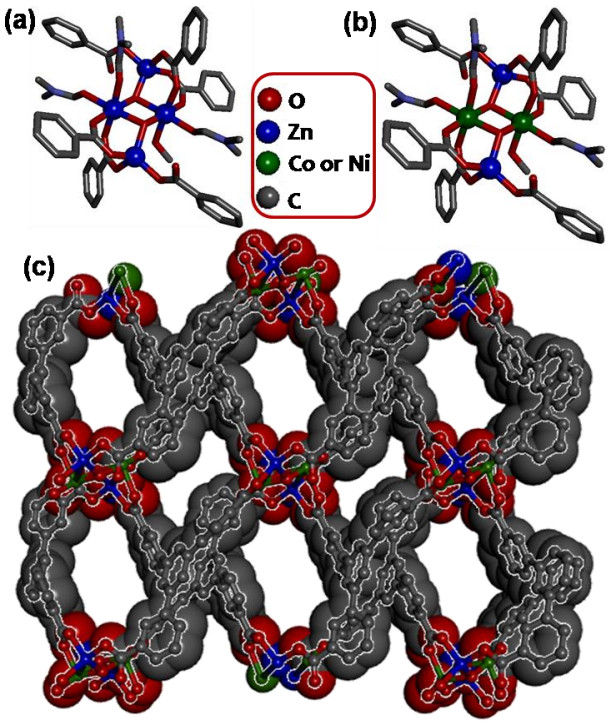

Figure 1. Single crystal X-ray structures showing co-ordination environment of (a) **PESD–1**⊃Guest, (b) **PESD–2**&**3**⊃Guest and (c) three-dimensional packing diagram of **PESD–2**&**3** viewed along the *b*-axis.

EDX-SEM and other Characterization

Energy-dispersive X-ray scanning electron microscope (EDX-SEM) analysis on single crystals in degassed phases **PESD–2** and **PESD–3** (Figure 2) indicated that the ratios of **Zn** and **Co** or **Ni** are almost equal, which agree with those obtained by XRF analysis. Moreover, EDX-SEM analysis also confirmed that, **Zn** and **Co** (or **Ni**) X-ray maps distributed uniformly throughout each single crystal and hence the **Zn** and **Co** (or **Ni**) metal ions presented in the same PCP particles, but not the physical mixture of those PCPs formed with **Zn** and **Co** (or **Ni**) individually, which agree with single crystal XRD analysis. Powder X-ray diffraction (PXRD) patterns (Figure S4) of **PESD–2**&**3**⊃Guest are similar to that of **PESD–1**⊃Guest, indicating that they are iso-structural. Moreover, these PXRD patterns of the as-synthesized phase are reasonably agreement with their simulated patterns, indicated that the samples produced by all the different synthetic methods were pure homogeneous in nature (Figure S5). Upon degassing of **PESD–2**&**3**⊃Guest at 250 °C, their PXRD patterns indicated that they are crystalline in the degassed phases and similar to those of **PESD–1** degassed (Figure S6). As a result, we could conclude that these three PCPs were isostructural frameworks not only in as-synthesized phase but also in degassed phase too. However, their crystallinity was slightly decreased, but the major peaks are reasonably matched with simulated peaks based on the degassed crystal structure model of **PESD–1**. Thermo-gravimetric analysis (TGA) measured for **PESD–2**&**3**⊃Guest under flowing N_2 with a flow rate of 10 °C /min (Figure S7). Coordination-free solvent molecules removed below 135 °C for the two compounds. Whereas, the coordinated DMF solvent molecules removed between 135 to 250 °C depending on the nature of the metal ions coordinated by DMF in the PCPs, to form degas phases similar to **PESD–1**. The essential point in these three, **PESD–1-3,** PCPs analogs exhibit dissimilarities in the releasing temperature of their coordinated solvents, indicating the interactions between the OMSs and coordinated guest molecules were conspicuously different. The observed weight loss was around 29 % for all the phases, which is in good agreement with expected value of 30 %. The onset of decomposition is around 400 °C for all the PCPs. Their thermal stability depends on the metal present in the oxo-cluster, $[Zn_2M_2((\mu_3\text{-}OH)_2]^{6+}$, and **PESD–2** is the most stable compared with other two analogs. Overall the present PCPs possess better thermal stability, compared with M_4O cluster contained in MOFs (~350 °C).[10]

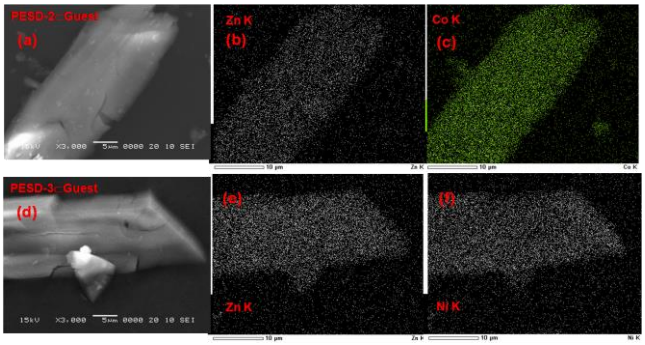

Figure 2. SEM and EDAX images of **PESD–2**⊃Guest (**a**, **b** and **c**) and **PESD–3**⊃Guest (**d**, **e** and **f**), respectively.

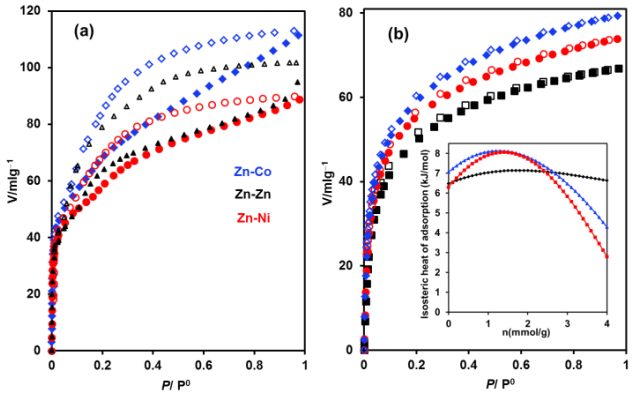

Figure 3. Adsorption isotherms of three analogs **PESD–1, 2** and **3**, for (a) CO_2 at 195 K and (b) H_2 at 77 K. Filled and open symbols represent adsorption and desorption data, respectively. The inset shows isosteric heats of H_2 adsorptions plotted by the viral equation.

Adsorption Study

The porosity of series of **PESD–1, 2** and **3**, ascertained from a type-I isotherm using CO_2 adsorption isotherms at 195 K (Figure.3). They did not adsorb N_2 at 77 K, probably owing to micro-porous blocking effect at such a very low temperature. The BET surface areas were 295, 317 and 272 m^2g^{-1} and Langmuir surface areas were 570, 662 and 560 m^2g^{-1} based on CO_2 adsorption isotherms, respectively for **PESD–1, 2** and **3**. The isosteric heats of H_2 adsorptions were -7.15, -8.13, and -8.05 kJ mol^{-1}, respectively for **PESD–1, 2** and **3** calculated based on the viral equation with the data obtained at 77 K and 87 K (inset in Figure3). As predicted, composite **PESD–2&3**, PCPS exhibits better surface area and heats of adsorption compared to **PESD–1 (Zn)** analogue. Among them, **PESD–2 (Co** analogue) displays highest surface area and heat of adsorption. Moreover, isosteric heats of H_2 adsorptions values are also high compare to many MOFs (for MOFs usually in the range from -4 to -7 kJ mol^{-1}),[10] which could be due to OMSs present in **PESD** PCPs. The mechanism of OMSs and gas adsorption phenomenon in theses bimetallic analogs could be explained as follows. The OMSs to the guest interaction basically depends on electronegativity of the metals or metal ions including the number of OMSs presents per metal ion. In our present study, all the three compounds, **PESD–1-3 (Zn-Zn, Zn-Co,** and **Zn-Ni)** containing a similar metal cluster of $[Zn_4O]^{6+}$ **(PESD–1)** and the composite cluster $[Zn_2M_2O]^{6+}$ (**M** = **Co** or **Ni**) **(PESD–2 & 3)** in the degassed state. Moreover, all the three compounds are isostructural, the number of OMSs expected would be the same. The main difference is at the metal cluster core part, where octahedral coordinated **Zn** metal replaced with **Co** (or **Ni**), respectively for, **PESD–2 & 3 (Zn-Co**, and **Zn-Ni)** analogs (Scheme 1). As observed in TGA, the coordinated DMF solvent molecules leave at ~173, ~189 and ~231 ° C, respectively for **Zn, Co,** and **Ni (PESD–1, 2,** and **3)** analogs. This is in good agreeing with their respective electronegativity values 1.65, 1.88 and 1.91, respectively for **Zn**, **Co**, and **Ni** metals. Moreover, the isosteric heats of H_2 adsorptions values also reasonably agree with the TGA data and electronegativity values. However, in case of **Ni (PESD–3)** analog, the isosteric heats of H_2 adsorptions and also adsorption of other gases are slightly lower than **Co (PESD–2)** analog, is due to low crystallinity observed for the degassed state (figure S6).

Superhydrophobicity and their Temperature Dependent Stability Study

Contact angle measurements were performed on powdered samples of the three *iso*-structural analogs, **PESD– 1, 2** and **3,** to estimate their superhydrophobic behavior. The measurements carried out at various possible high temperatures on as-synthesized and as well as degassed samples separately. The contact angles measured on as-synthesized powder samples at room temperature (~ 30 ° C) of **PESD– 1, 2** and **3**, respectively were 155.5 °, 159.3 ° and 160.8 ° (Figure. 4 and 5 & S9-S10). Similarly, the contact angles measured at RT on degassed samples were 158.4 °, 157.6 °, and 158.8 °, respectively for **PESD– 1, 2** and **3** (Figure. S11). Moreover, the roll-off angles observed as less than 10 °, for all the three analogs, indicative of a superhydrophobic surface[13] (Lotus behavior or self-cleaning). It noteworthy point could be, the MOFs/PCPs family[10] of archetypal framework $[Zn_4O(L)_n]$ formed similar chemical formula of H_3**BTB** ligands with coordinating ($RCOO^-$) moiety at *para*-position and other[6] are hygroscopic in nature. However, similar contact angle measurements[7b] on the powdered samples of pure H_3**BTMB** ligand alone did not have any contact angle, indicated that the ligand alone in uncoordinated state is hydrophilic in nature.

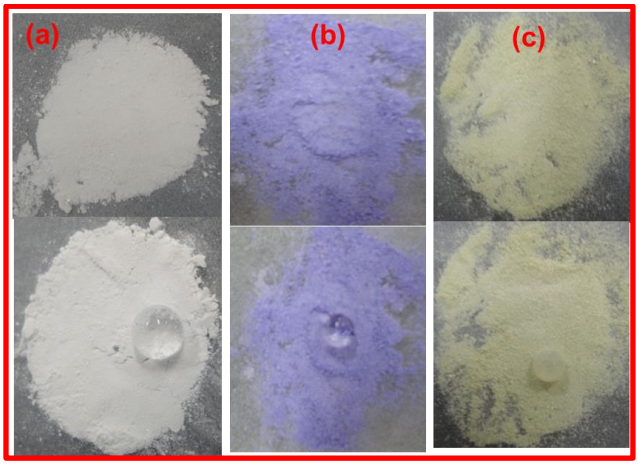

Figure 4. Pictures showing three analogs of powder samples and a drop of water placed on them for **PESD–1** (**a**), **PESD–2** (**b**) and **PESD–3** (**c**), respectively.

The study about the superhydrophobic effect on the particle size and their hierarchical roughness revealed that the contact angles decreased with increasing the particle size from a powder to pellet form (Fig 5 and 6), similar to our previous study[7a] (Cassie- Baxter model of superhydrophobicity). Moreover, we also carried out contact angle measurements on the powder samples of **PESD– 1, 2** and **3**, at different temperatures starting from RT to 90 ° C, by varying 10 ° C temperature intervals for each measurement (Figure. 5 and Figure. S9 & S10). As shown in figure 5 for **PESD–3** compound, all the powder samples showed high contact angles even at a high temperature for longer time periods. This is evident that the present composite PCPs displayed stable hydrophobic nature survives even at high temperature. However, as expected the contact angles were slightly decreased at high temperature. It could be due to water vapor started condensing near to its boiling point by reducing the roughness of the surface similar to lotus leaf.[14] Indeed, at high temperature, most of the superhydrophobic PCPs including lotus leaf[14] could not preserve their hydrophobic surface. From the above observations, we conclude that this unique superhydrophobic behavior might be due to; these PCPs (**PESD-1, 2** and **3**) have a strong affinity towards the air (or gas molecules) between the layers due to strong OMSs. The gaseous molecules (or air) repel the liquid water without penetrating into the layers (Cassie- Baxter model of superhydrophobicity). In fact, even as synthesized single crystal state, **PESD-1, 2** and **3,** PCPs lose some of the un-coordinated solvent molecules immediately in the open atmosphere and replace with atmosphere gaseous molecules (or air). Due to the above unique behavior, the current PCPs, **PESD-1, 2** and **3,** are superhydrophobic in all the synthesized states (powder

and single crystals) and degassed state, including at high temperatures (RT to 90 ° C).

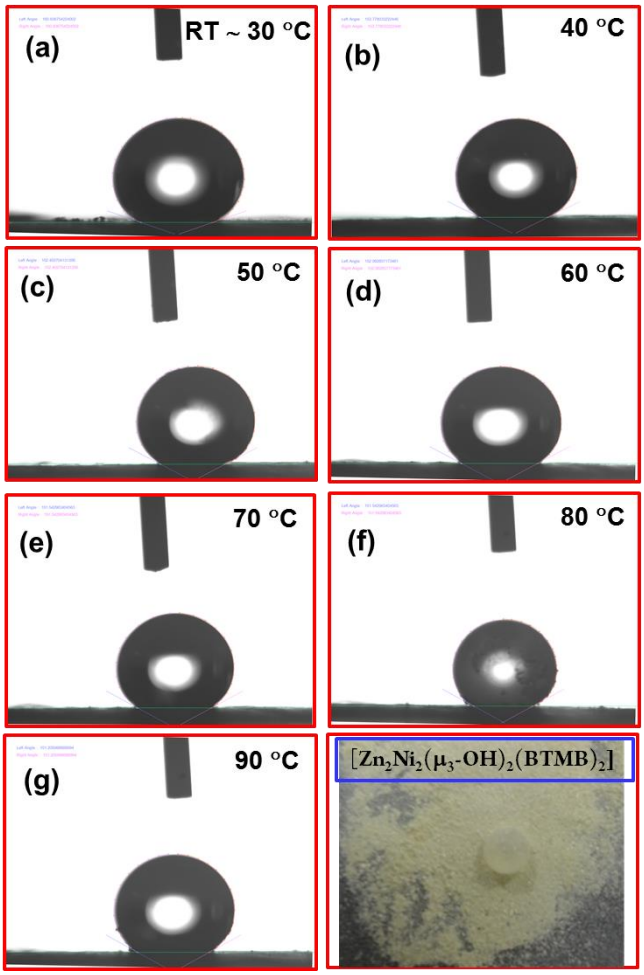

Figure 5. Pictures showing contact angles measured on powdered samples of **PESD–3**, at various temperatures starting for at room temperature (~ 30 ° C) (**a**) to at 90 ° C (**g**).

Aromatic Solvent Selectivity and Oil Spill Cleanup Study

We also examined the sorption ability of two iso-structural **PESD-2** & **3** analogs, by taking as model study for three different six-membered-ring organic solvents with similar molecular size, but differ in polarity like aromatic and aliphatic solvents. The adsorption profiles of **PESD-2** & **3** measured at 298 K on degassed samples using three different solvents (benzene, toluene and cyclohexane) displayed in figure 6 (a) and (b). Surprisingly, the adsorption isotherms for aromatic solvents (benzene and toluene) displayed a gate-opening profile and enter the solvent molecules into the pores. Whereas, the aliphatic solvent molecules (cyclohexane) displayed gate closing behavior and could not enter in to the pores. This could be due to aliphatic organic solvents excluded from the pores by corrugated and terminated aromatic hydrocarbon moieties towards the solvent interactive surface. These results clearly indicated that, **PESD-2** & **3** exhibits size, shape and surface interactions toward guest molecules. Moreover, these experiments clearly demonstrated that **PESD-2** & **3** can accommodate a variety of aromatic solvents. Among all the **PESD-1, 2** and **3**, analogs, **PESD-2 (Co)** composite **PCP** shows highest adsorption capacity of benzene and toluene solvent, this is agree with their surface area and heats of adsorption values of these analogs.

For real-time applications of present composite superhydrophobic PCPs, we also carried out oil spill cleanup study for **PESD-2** & **3**. In fact, the powder samples showed superhydrophobicity with contact angles > 150 ° (155.5 °, 159.3 ° and 160.8 °, respectively for **PESD– 1, 2** and **3**) were converted into pellets (hydrophobic surfaces observed in the pellet-disk form) of **PESD-2** & **3** for oil cleanup study. Pellets of **PESD-2** & **3**, were placed within a mixture consisting of an organic solvent/oil and water. Outstandingly, the pellets floated on the water surface and adsorbed organic solvents/oils selectively from the water (Figure 6; see movie files **1** – **3**, in the SI). More precisely and quantitatively, 150 mg and 135 mg of **PESD-2** & **3** pellet discs with surface areas of ~1.7 5 cm^2 and ~1.5 cm^2 could uptake ~350 wt% and ~385 wt% of olive oil, respectively. Moreover, these samples could be reusable for several cycles without losing its crystallinity and superhydrophobicity. These results evidenced that **PESD-2** & **3** utilized the pores depending on the solvent, conditions used, along with the regular capillary action utilized by non-porous materials. Hence, the amount of absorbed solvent could be several times larger than the conventional non-porous superhydrophobic solids[15], which just utilize the capillary action in the organic solvents/ oil spill clean-up process.

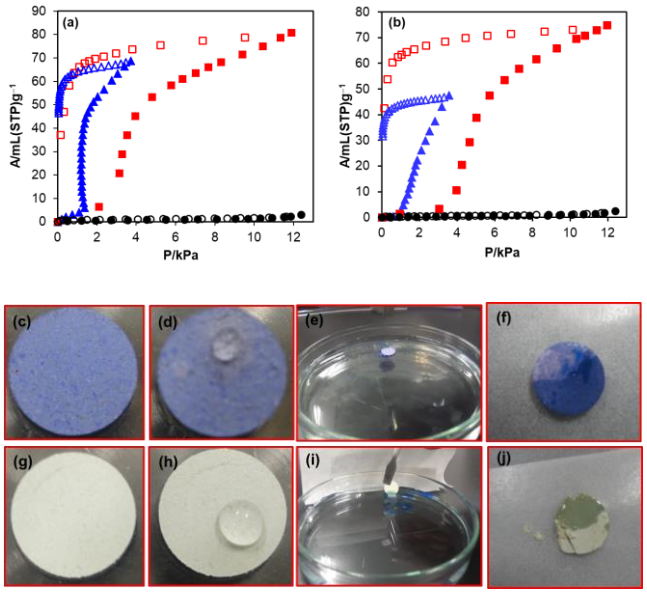

Figure 6. (Top) Adsorption isotherms of **PESD-2** (a) and **PESD-3** (b) recorded for benzene (red squares), toluene (blue triangles), and cyclohexane (black circles) at 298 K. Filled and open symbols represent adsorption and desorption data, respectively. (Bottom) pictures showing pellet form, water droplet placed on pellet, PCP pellet adsorbing oil on water surface and oil adsorbed pellet for **PESD-2** (c-f) and **PESD-3** (g-j), respectively.

CONCLUSIONS

In conclusion, we described a new *de nova* synthetic method for the synthesis of superhydrophobic composite PCPs with interesting stable bimetallic oxo-clusters. For this purpose, we utilized coordination priorities of first row transition elements and achieved $[\mathbf{Zn_2M_2O}]^{6+}$ (**M** = **Co** or **Ni**) clusters, in which substitution of $\mathbf{Co^{2+}}$ or $\mathbf{Ni^{2+}}$ at an octahedral-coordinated $\mathbf{Zn^{2+}}$ position. As designed, these new composite **PCPs** shown, noticeably different coordination affinities with solvent molecules in raw phases converted to OMSs in their degassed phases. Furthermore, these interesting composite PCPs, exhibits incredible superhydrophobic properties with contact angles > 150 ° even at high temperature, compared to conventional superhydrophobic materials. Fascinatingly, these new PCPs display selective adsorption towards aromatic solvents like benzene and toluene over aliphatic solvents like cyclohexane. Among all the **PESD-1, 2** and **3**, analogs**, PESD-2 (Co)** composite PCP shows the highest surface area, iso-steric heats of adsorptions and solvent adsorption capacity *etc*. They also exhibit oil spill cleanup from the water surface in the powder form as well as pellet form. This study certainly provides a roadmap for engineering new composite porous materials for better water and thermal stability with possibly of containing more OMSs for applications in catalysis and separation technology. In our next study, we report exciting results about water stable green heterogeneous catalytic properties of these fascinating composite superhydrophobic PCPs.

EXPERIMENTAL SECTION

Materials. $Zn(NO_3)_2{\cdot}4H_2O$ and methanol (MeOH) purchased from Merck and $Co(NO_3)_2{\cdot}6H_2O$, $Ni(NO_3)_2{\cdot}6H_2O$, and *N*, *N*-dimethylformamide (DMF) purchased from Sigma Aldrich, USA, used as received without further purification.

Synthesis and Characterization of PESD−2⊃Guest. In a 2-mL glass vial containing 1 mL mixed solvent of DMF/MeOH/H_2O (2:1:1), a solid mixture of ligand H_3BTMB (11 mg, 0.025 mmol), $Co(NO_3)_2{\cdot}6H_2O$ (10.9 mg, 0.038 mmol) and $Zn(NO_3)_2{\cdot}4H_2O$ (6.54 mg, 0.025 mmol) dissolved. To this reaction mixture, 20 µL deprotonating reagent of NaOH (0.01 M) added. After adding NaOH, the reaction mixture converted as violet color precipitation with initial pH of ~ 6.0. The entire reaction mixture heated in a temperature-controllable oven from RT (~ 30 ° C) to 100 °C, over a period of 4 h. Later, the reaction mixture heated at a constant temperature of 100 ° C for a period of 48 h. Finally, the reaction mixture cooled from 100 ° C to RT (~ 30 ° C) over a period of 6 h. The product contains homogeneous violet color flake type crystals, which were isolated by washing with MeOH and air-dried. The yield: 17.5 mg, 86% observed based on 1 mole of H_3BTMB. Elemental micro-analysis for **PESD−2⊃**Guest, $[Zn_2Co_2(\mu_3\text{-}OH)_2(BTMB)_2(DMF)_3(MeOH)]\cdot(DMF)_2(H_2O)_2(MeOH) \equiv C_{71}H_{79}N_5O_{23}Zn_2Co_2$, calculated (%): C, 52.67; H, 4.92; N, 4.33. Found (%): C, 52.23; H, 5.15; N, 4.10. FT-IR (4000-525 cm^{-1}): 3616 (s, w), 3381 (br, w), 3061 (s, w), 2931 (s, w), 1649(vs), 1609 (vs), 1588 (s), 1568 (vs), 1495 (w), 1441 (m), 1413 (m), 1373 (vs), 1263 (m), 1247 (m), 1157 (w), 1105 (m), 1077 (m), 1055 (w), 1028 (m), 876 (m), 802 (s), 761 (vs), 715 (m), 693 (s), 686 (s), 680 (vs), 653 (m).

Synthesis and Characterization of PESD−3⊃Guest. Similarly, a solid mixture of H_3BTMB (11 mg, 0.015 mmol), $Ni(NO_3)_2{\cdot}6H_2O$ (10.9 mg,0.038 mmol) and $Zn(NO_3)_2{\cdot}4H_2O$ (6.54 mg,0.025 mmol) dissolved in a 1 mL mixed solvent of DMF/MeOH/H_2O (2:1:1) in an 2-mL glass vial. Other synthetic conditions used like that employed for **PESD−2⊃Guest**. The final product contains homogeneous light green color flake type crystals, which isolated by washing with MeOH and air-dried. The yield: 15.5 mg, 76% observed based on 1 mole of H_3BTMB. Elemental micro-analysis for **PESD−3⊃**Guest**,** $[Zn_2Ni_2(\mu_3\text{-}OH)_2(BTMB)_2(DMF)_3(MeOH)]\cdot(DMF)_2(H_2O)_2(MeOH) \equiv C_{71}H_{79}N_5O_{23}Zn_2Ni_2$, calculated (%): C, 52.69; H, 4.92; N, 4.33. Found (%): C, 52.31; H, 5.25; N, 4.17. FTIR (4000-525 cm^{-1}): 3618 (s, w), 3373 (br, w), 3061 (s, w), 2932 (s, w), 1648(vs), 1611 (vs), 1588 (s), 1568 (vs), 1494 (w), 1440 (m), 1414 (m), 1372 (vs), 1268 (m), 1253 (m), 1158 (w), 1106 (m), 1079 (m), 1058 (w), 1028 (m), 876 (m), 803 (s), 761 (vs), 716 (m), 695 (s), 690 (s), 681 (vs), 653 (m).

Large Scale Syntheses of PESD−2⊃Guest & PESD−3⊃Guest. Syntheses of large-scale products of both **PESD−2⊃Guest** & **PESD−3⊃Guest** achieved by similar solvo-thermal condition method using Teflon lined autoclave (See SI for more details).

General Characterization Techniques. Thermo-gravimetric analyses (TGA) carried out using a Hitachi STA 7200 under N_2 flow with 10 K min^{-1} ramp rate. The Powder X-ray diffraction (PXRD) patterns recorded using a Rigaku RINT powder X-Ray diffractometer with using *Cu* K_a radiation. Single crystal X-ray diffraction measurements performed at 223 K with a Rigaku AFC10 diffractometer with Rigaku Saturn Kappa CCD system equipped with a MicroMax-007 HF /Vari-Max rotating-anode X-ray generator with confocal monochromatic *MoKa* radiation. Gas adsorption isotherms carried out using Belsorp Mini volumetric adsorption instrument, BEL JAPAN INC, Japan. X-ray florescence analysis carried out by using RIGAKU EDXL-300, Japan. FTIR spectra were recorded at 298 K temperature by using Cary 639 FTIR with Diamond ATR, Agilent technologies, USA. SEM/EDX analysis carried out using JEOL, JED-2300.

Contact Angle Measurements. Contact angels were measured[7b] on powder samples using HOLMARC contact angle meter with the rotatable substrate holder, temperature controller and automated water dispenser unit, Model No: HO-IAD-CAM-01B, Holmarc Opto-Mechtronics LTD, India. To perform contact angle measurements, the powder samples ~ 30 mg of **PESD− 1, 2** and **3** were deposited on an aluminum substrate bed. Using a glass slide the powder samples pressed to make flat surface. 20 µL of water droplet released slowly on the flat surface of the powder samples using automated 100 µL water dispenser unit. Later, the droplet image captured using high performance charge-coupled device (CCD) sensor. *B*-spline drop snake analysis used to perform analysis of the contact angles of all the powder samples. Similarly, temperature dependent contact angles were also measured[7b] at room temperature (~ 30 ° C) to 90 ° C by varying 10 ° C step intervals. To achieve these high temperatures the substrate bed heated with the help of temperature controller equipment. At high temperature, the contact angles measured relatively quickly (~3 min) after dropping the water droplet due to water evaporation problem.

Oil Spill Cleanup Study. Removing organic solvents and oil spills from water surface experiments carried out by converting powder samples of **PESD− 2** and **3,** into pellet disc (~2.2 cm^2 area) by applying 4~6 MPa pressure. The organic solvents like toluene, hexane, benzene and olive oil *etc.* labeled with Oil Blue 35 (to distinguish colorless oils from colorless water) dropped in water containing petri dish. Pellet discs of **PESD− 2** and **3**, dropped in the middle of the organic solvent or oil drop on the water surface. After the pellet discs adsorbed organic solvent or oil drop, the adsorbed samples removed from the water surface and same samples were used for quantitative analysis and other characterizations.

ASSOCIATED CONTENT

Supporting Information

Supporting information material is available free of charge via the Internet at "http://pubs.acs.org."

Additional information about syntheses, X-ray refinement data, TGA, FTIR, PXRD, Adsorption study, iso-steric heats of H_2 adsorptions, contact angles and oil-spill cleanup movie files (1-3) etc.

Crystallographic information files (CIFs) for **PESD−2⊃Guest**, CCDC **1854846** and for **PESD−3⊃Guest**, CCDC **1854847**.

AUTHOR INFORMATION

Corresponding Author

*E-mail: kitagawa@icems.kyoto-u.ac.jp and kprao2005@gmail.com

ACKNOWLEDGMENT

K. P. R Acknowledges DST-SERB, for financial support grant no: EMR/2014/001114, for early career award. J. S Acknowledges DST-SERB for JRF fellow ship.

REFERENCES

(1) (a) Yaghi, O. M.; 'Keeffe, M. O.; Ockwig, N. W.; Chae, H. K.; Eddaoudi, M.; Kim, J. *Nature.* **2003**, *423*, 705-714. (b) Kitagawa, S.; Kitaura, S. R.; Noro, S. -I. *Angew. Chem. Int. Ed.***2004**, *43*, 2334-2375. (c) Long, J. R.; Yaghi, O. M. *Chem. Soc. Rev.* **2009**, *38*, 1213-1214. (d) Férey, G. *Chem. Soc. Rev.* **2008**, *37*, 191-214. (e) Tan, J. C.; Cheetham, A. K. *Chem. Soc. Rev.* **2011**, *40*, 1059-1080. (f) Li, J. –R.; Sculley, J.; Zhou, H. –C. *Chem. Rev.* **2012**, *112*, 869-932. (g) Suh, M. P.; Park, H. J.; Prasad, T. K.; Lim, D. –W. *Chem. Rev.* **2012**, *112*, 782-835. (h) Shimizu, G. K. H.; Vaidhyanathan, R.; Taylor, J. M. *Chem. Soc. Rev.* **2009**, *38*, 1430-1449. (i) Lee, J.; Farha, O. K.; Roberts, J.; Scheidt, K. A.; Nguyen, S. T.; Hupp, J. T. *Chem. Soc. Rev.* **2009**, *38*, 1450-1459. (j) Lian, X.; Fang, Y.; Joseph, E.; Wang, Q.; Li, J.; Banerjee, S.; Lollar, C.; Wang, X.; Zhou, H. -C. *Chem. Soc. Rev.* **2017**, *46*, 3386-3401. (k) Liu, S. -Y.; Zhou, D. -D.; He, C. -T.; Liao, P. -Q.; Cheng, X. -N.; Xu, Y. -T.; Ye, J. -W.; Zhang, J. -P.; Chen, X. -M. *Angew. Chem. Int. Ed.* **2016**, *55*, 16021-16025.

(2) (a) Wang, Z.; Cohen, S. M. *Chem. Soc. Rev.* **2009**, *38*, 1315-1329. (b) Dolgopolova, E. A.; Ejegbavwo, O. A.; Martin, C. R.; Smith, M. D.; Setyawan, W.; Karakalos, C. H.; Henager, S. G.; Loye, H. –C. Z.; Shustova, N. B. *J. Am. Chem. Soc.***2017**, *139*, 16852–16861. (c) Gonzalez, M. I.; Kapelewski, M. T.; Bloch, E. D.; Milner, P. J.; Reed, D. A.; Hudson, M. R.; Mason, J. A.; Barin, G.; Brown, C. M.; Long, J. R. *J. Am. Chem. Soc.* **2018**, *140*, 3412−3422. (d) Diercks, C. S.; Liu, Y.; Cordova, K. E.; Yaghi, O. M. *Nat Mater.* **2018**, *17*, 301-307. (e) Koo, J.; Hwang, I. –C.; Yu, X.; Saha, S.; Kim, Y.; Kim, K. *Chem. Sci.* **2017**, *8*, 6799-6803. (f) Kim, S. R.; Joarder, B.; Hurd, J. A.; Zhang, J.; Dawson, K. W.; Gelfand, B. S.; Wong, N. E.; Shimizu, G. K. H. *J. Am. Chem. Soc.* **2018**, *140*, 1077−1082.

(3) (a) Das, S.; Kim, H.; Kim, K. *J. Am. Chem. Soc.* **2009**, *131*, 3814-3815. (b) Zheng, S. –T.; Wu, T.; Zuo, F.; Chou, C.; Feng, P.; Bu, X. *J. Am. Chem. Soc.* **2012**, *134*,1934-1937. (c) Rao, K. P.; Vidyavathy, B.; Minimol, M. P.; Vidyasagar, K. *Inorg. Chem.* **2004**, *43*, 4610-4614. (d) Ziebel, M. E.; Darago, L. E.; Long, J. R. *J. Am. Chem. Soc.* **2018**, *140*, 3040−3051. (e) Denny, M. S.; Parent, L. R.; Patterson, J. P.; Meena, S. K.; Pham, H.; Abellan, P.; Ramasse, Q. M.; Paesani, F.; Gianneschi, N. C.; Cohen, S. M. *J. Am. Chem. Soc.* **2018**, *140*, 1348-1357. (f) Wang, T.; Kim, H. –K.; Liu, Y.; Li, W.; Griffiths, J. T.; Wu, Y.; Laha, S.; Fong, K. D.; Podjaski, F.; Yun, C.; Kumar, R. V.; Lotsch, B. V.; Cheetham, A. K.; Smoukov, S. K. *J. Am. Chem. Soc.* **2018**, *140*, 6130–6136.

(4) Schnobrich, J. K.; Lebel, O.; Cychosz, K. A.; Dailly, A.; Wong-Foy, A. G.; Matzger, A. J. *J. Am. Chem. Soc.* **2010**, *132*, 13941-13948.

(5) Park, K. S.; Ni, Z.; Côte, A. P.; Choi, J. Y.; Huang, R.; Uribe-Rome, F. J.; Chae, H. K.; 'Keeffe, M. O.; Yaghi, O. M. *PNAS.* **2006**, *103*, 10186-10191.

(6) (a) Rao, K. P.; Higuchi, M.; Duan, J.; Kitagawa, S. *Cryst. Growth Des.* **2013**, *13*, 981-985. (b) Zheng, S. –T.; Wu, T.; Zuo, F.; Chou, C.; Feng, P.; Bu, X. *J. Am. Chem. Soc.* **2012**, *134*,1934-1937.

(7) (a) Rao, K. P.; Higuchi, M.; Sumida, K.; Furukawa, S.; Duan, J.; Kitagawa, S. *Angew. Chem., Int. Ed.* **2014**, 53, 8225-8230. (b) Rao, K. P.; Devi, Y. K.; Suryachandram. J.; Rao, R. P.; Behera. J. N. *Inorg. Chem.* **2017**, *56*, 11184-11189.

(8) (a) Chui, S. S. -Y.; Lo, S. M. -F.; Charmant, J. P. H.; Orpen, A. G.; Williams, I. D. *Science.***1999**, *283*, 1148-1150. (b) Ohmori, O.; Fujita, M. *Chem. Commun.* **2004**, 1586-1587. (c) Han, J. W.; Hill, C. L. *J. Am. Chem. Soc.* **2007**, *129*, 15094-15095. (d) Forse, A. C.; Gonzalez, M. I.; Siegelman, R. L.; Witherspoon, V. J.; Jawahery, S.; Mercado, R.; Milner, P. J.; Martell, J. D.; Smit, B.; Blümich, B.; Long, J. R.; Reimer, J. A. *J. Am. Chem. Soc.* **2018**, *140*, 1663–1673. (e) Dincă, M.; Long, J. R. *Angew. Chem., Int. Ed.* **2008**, *47*, 6766-6779. (f) Xiang, S.; Zhou, W.; Gallegos, J. M.; Liu, Y.; Chen, B. *J. Am. Chem. Soc.* **2009**, *131*, 12415-12419. (g) Wang, X. -S.; Meng, L.; Cheng, Q.; Kim, C.; Wojtas, L.; Chrzanowski, M.; Chen, Y. -S.; Zhang, X. P.; Ma, S. *J. Am. Chem. Soc.* **2011**, *133*, 16322-16325. (h) Flaig, R. W.; Popp, T. M. O.; Fracaroli, A. M.; Kapustin, E. A.; Kalmutzki, M. J.; Altamimi, R. M.; Fathieh, F.; Reimer, J. A. ; Yaghi, O. M. *J. Am. Chem. Soc.*, **2017**, *139*, 12125-12128.

(9) (a) Bloch, E. D.; Queen, W. L.; Krishna, R.; Zadrozny, J. M.; Brown, C. M.; Long, J. R. *Science.* **2012**, *335*, 1606-1610. (b) Yoon, M.; Srirambalaji, R.; Kim, K. *Chem. Rev.* **2012**, *112*, 1196-1231. (c) Diercks, C. S.; Lin, S.; Kornienko, N.; Kapustin, E. A.; Nichols, E. M.; Zhu, C.; Zhao, Y.; Chang, C. J.; Yaghi, O. M. *J. Am. Chem. Soc.* **2018**, *140*, 1116–1122. (d) Wang, Y.; Huang, N. –Y.; Shen, J. –Q.; Liao, P. –Q.; Chen, X. –M.; Zhang, J. -P. *J. Am. Chem. Soc.* **2018**, *140*, 38−41.

(10) (a) Chae, H. K.; Siberio-Pérez, D. Y.; Kim, J.; Go, Y. B.; Eddaoudi, M.; Matzger, A. J.; Keeffe, M. O.; Yaghi, O. M. *Nature.* **2004**, *427*, 523-527. (b) Furukawa, H.; Ko, N.; Go, Y. B.; Aratani, N.; Choi, S. B.; Choi, E.; Yazaydin, A. Ö.; Snurr, R. Q.; 'Keeffe, M. O.; Kim, J.; Yaghi, O. M. *Science.* **2010**, *329*, 424-428.

(11) He, Y.; Bian, Z.; Kang, C.; Cheng, Y.; Gao, L. *Tetrahedron.* **2010**, *66*, 3553-3563.

(12) Batten, S. R.; Robson, R. *Angew. Chem., Int. Ed.***1998**, *37*, 1460-1494.

(13) (a) Colombo, V.; Galli, S.; Choi, H. J.; Han, G. D.; Maspero, A.; Palmisano, G.; Masciocchi, N.; Long, J. R. *Chem. Sci.* **2011**, *2*, 1311-1319. (b) Chen, T. -H.; Popov, I.; Zenasni, O.; Daugulis, O.; Miljanic, O. S. *Chem. Commun.* **2013**, *49*, 6846-6848. (c) Wang, Z. Q.; Cohen, S. M. *Chem. Soc. Rev.* **2009**, *38*, 1315-1329. (d) Nguyen, J. G.; Cohen, S. M. *J. Am. Chem. Soc.* **2010**, *132*, 4560-4561. (e) Yang, C.; Kaipa, U.; Mather, Q. Z.; Wang, X. P.; Nesterov, V.; Venero, A. F.; Omary, M. A. *J. Am. Chem. Soc.* **2011**, *133*, 18094-18097. (f) Serre, C. *Angew. Chem., Int. Ed.* **2012**, *51*, 6048-6050. (g) He, C. –T.; Jiang, L.; Ye, Z. –M.; Krishna, R.; Zhong, Z. –S.; Liao, P. –Q.; Xu, J.; Ouyang, G.; Zhang, J. –P.; Chen, X. –M. *J. Am. Chem. Soc.* **2015**, *137*, 7217-7223. (h) Jayaramulu, K.; Datta, K. K. R.; Rösler, C.; Petr, M.; Otyepka, M.; Zboril, R.; Fischer, R. A. *Angew. Chem., Int. Ed.* **2016**, *55*, 1178-1182.

(14) Chenga, Y. –T.; Rodak, D. E. *Appl. Phys. Lett.* **2005**, *86*, 144101-144103.

(15) Yuan, J.; Liu, X.; Akbulut, O.; Hu, J.; Suib, S. L.; Kongi, J.; Stellacci, F. *Nature nano.* **2008**, *3*, 332-336.

SYNOPSIS TOC